ANNUAL TRANSACTIONS OF THE NORDIC RHEOLOGY SOCIETY, VOL. 16, 2008

Thixotropy in Water-Based Drilling Fluids

Ahmadi Tehrani

M-I SWACO Research and Technology Centre, Aberdeen, United Kingdom

ABSTRACT

Rheology of drilling fluids affects the frictional pressure drop and the solids carrying capacity of the fluids during the drilling operation. Drilling fluid rheology is commonly controlled by using a variety of clay or polymeric materials, depending on the type of fluid used and the demands of the specific drilling operation. Most drilling fluids possess varying degrees of time- and shear-dependent thixotropic properties. Among them, water-based fluids containing clays, such as bentonite, exhibit a pronounced thixotropic behaviour. This characteristic can have a significant effect on the peaks and troughs of pressure that occur in the wellbore when the drillstring or the tool-string is moved in and out, or when pumping starts after a break in circulation. Major pressure fluctuations can lead to fracturing of the formation, loss of circulation, influx of formation fluids into the wellbore, or collapse of the wellbore. Thus, a practical means of accounting for thixotropy in hydraulics calculations would be of great value for maintaining safety as well as the integrity of the wellbore.

As far as can be determined the thixotropic characteristics of drilling fluids have not been quantified for engineering applications. In this work, a simple model based on the concept of a structure parameter is used to describe drilling fluid thixotropy. Empirical relationships are devised that can predict, with good approximation, the time- and shear-dependence of rheological parameters within the range of shear rates encountered in the drillstring and in the annulus between the drillstring and the borehole wall. The model shows potential for use in calculation of drilling hydraulics.

INTRODUCTION

The function of a drilling fluid is to cool and lubricate the drill bit, transport cuttings to the surface, and stabilise the wellbore. For the fluid to perform satisfactorily, frictional pressure drop and solids-bearing capacity must be maintained at an optimum level throughout the drilling operation. The rheological parameters that control these properties are the fluid viscosity and the yield stress. Efficient pumping requires a low enough viscosity while adequate yield stress is needed to maintain cuttings in suspension, particularly during circulation breaks.

Drilling fluid rheology is commonly controlled by using a variety of clay or polymeric materials, depending on the type of fluid used and the demands of the specific drilling operation. Of the various types of drilling fluids, water-based fluids (also referred to as water-based mud, WBM) containing clays such as bentonite (or particulates such as mixed metal oxides or hydroxides) exhibit a pronounced thixotropic behaviour. The clay-based fluids are suspensions of bentonite in water to

which various compounds such as heavier minerals, polymers and surfactants are added to control density, rheology and fluid loss, and to improve other fluid properties such as shale inhibition and lubricity. The suspended clay particles are thin, flat platelets that are electrically charged and interact to form a loose house-of-cards structure that is responsible for the gelling characteristics of the fluid when at rest, and its thinning behaviour when sheared.[1] This structure and the resulting bulk rheological properties are time- and shear-history dependent and the fluid is said to possess thixotropy properties.

The rheological properties of the drilling fluid are subject to continuous modification as the fluid travels around the wellbore. This includes changes caused by variations in shear rate, temperature, pressure, as well as chemical modification of the fluid as it contacts various formations on its way to the surface. In addition, mechanical and thermal stresses that lead to the degradation of the drilling fluid additives can cause significant changes in fluid rheology.[2]

The shear rates to which the fluid is subjected can range from around 10^3 s^{-1} in the drillstring (as the mud travels down the well), to ~10^5 s^{-1} in the highly turbulent flow as the fluid issues from the drill bit, to those prevalent in the annulus, *i.e.* 0-10^2 s^{-1} (depending on the eccentricity of the annular space), as it carries the drill cuttings to the surface.

The combination of temperature, pressure, composition, time- and shear-history dependence of the bulk rheological properties makes a full characterisation of the drilling fluid rheology a complex task. A number of works have been reported on the temperature, pressure and composition dependence of water-based drilling fluids,[2-5] but only few references exist in the literature on attempts to quantify the thixotropic behaviour of such fluids. Mercer and Weymann[6] investigated the time dependence of viscosity in bentonite-water suspensions and observed that it can be described by a double-exponential function. More recently, Dolz *et al.*[7] investigated the thixotropic behaviour of water-based drilling fluids containing bentonite, at 6-12% (w/w) concentration, and a polymeric material. They found that the lower concentrations of bentonite produced the greatest thixotropic effect. They obtained an empirical equation that relates shear stress to the concentrations of the thickeners, the shear rate and the formulation stirring time.

As far as can be determined, the thixotropic characteristics of drilling fluids have not been quantified for engineering applications. To improve the quality of downhole predictions, there is a need for some form of engineering relationship that can describe the time- and shear-history dependence of rheological properties in drilling fluids. Currently, some of the more advanced hydraulics modelling calculations account for this effect by using the so-called "gel" values that are measured by the API-standard oilfield viscometric method. In this method, the shear stress of the fluid is measured after a 10-second, 10-minute, and sometimes 30-minute rest period following a short interval of shearing at a high rate. A requirement of this approach has been for the design of fluids with non-progressive gels, *i.e.* where the longer-term gels are not significantly higher than the 10- or 30-minute gel values. This approach has proved to be adequate for the applications encountered to date. However, as drilling scenarios become more complex, a need for a better way of accounting for thixotropy of drilling fluids will inevitably arise. An example of this is in depleted-zone drilling where the operating window for fluid density (mud weight), between the maximum and minimum dictated by the pore pressure and fracture gradient considerations, becomes very narrow. In such circumstances, more precise knowledge of fluid thixotropy may help to better control drilling hydraulics.

The work reported here uses a simple model based on the concept of a structure

parameter to describe drilling fluid thixotropy. Empirical relationships are devised that can predict, with good approximation, the time- and shear-dependence of rheological parameters within the range of shear rates encountered in the drillstring and the annulus. The model requires further development but shows potential for use in drilling hydraulics calculations.

THIXOTROPIC FLOW BEHAVIOUR

Thixotropic materials are fluids containing some form of structure as a result of formation of flocs or aggregates between suspended particles or moieties. In clay suspensions the formation of structure is promoted by increased encounter between suspended particles, which can result from Brownian motion of the particles or from the velocity gradient when the bulk of the material is sheared. Structure breakdown can be due to collision of particles and flocs as well as viscous drag exerted by the liquid medium when the material is sheared. On a smaller scale, the Brownian motion of primary particles making up a floc can also cause floc breakup. This means that under certain conditions both Brownian motion and shear can cause structure breakdown. Thixotropic behaviour occurs when the buildup effect of Brownian motion is dominant over the breakdown effect of shear.

When a thixotropic material is sheared, the buildup and breakdown processes compete and a dynamic equilibrium eventually results. Since the rates of buildup and breakdown of structure are finite, if conditions are displaced from equilibrium (*eg.* by a change in shear rate), the structure level will take some time to adjust. The change in structure will be detected by a corresponding change in shear stress. This is illustrated in the shear rate step-change experiments of Fig. 1.

Thixotropic behaviour may also be observed by ramping the shear rate up or down and recording the resulting changes in shear stress, Fig. 2. The breakdown of structure, which occurs as shear rate is increased along the "up" curve, is not fully recovered during the "down" curve and the material completes the cycle with some residual broken structure. The area enclosed between the "up" and "down" curves (the hysteresis loop) is an indication of the extent of thixotropy of the material.

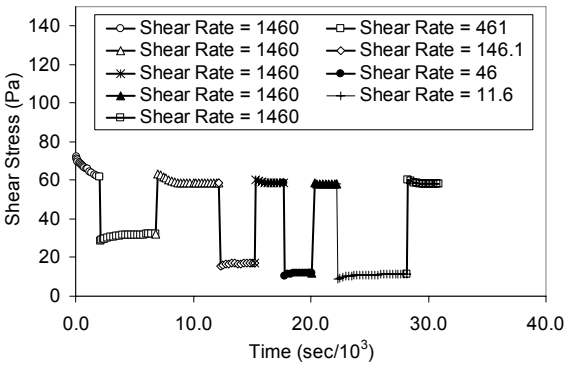

Figure 1. Shear rate step-change tests.

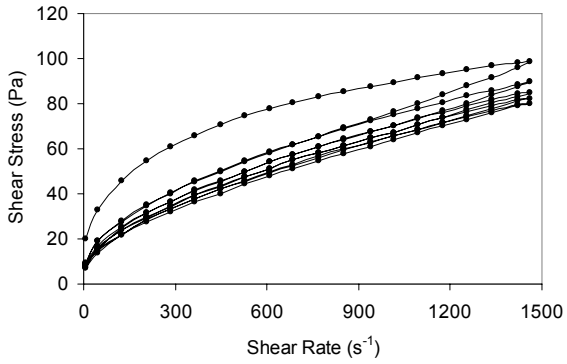

Figure 2. Hysteresis loops demonstrating thixotropic behaviour.

If the material is now left to rest, the broken structure will gradually re-form. However, if it is subjected to successive ramping cycles until two consecutive loops superpose, then there is no further drop in the level of structure and the loop is called the equilibrium loop. Another characteristic of such rheograms is the equilibrium flow curve. This is obtained by allowing the material to reach equilibrium structure level at each new shear rate such that the "up"

and "down" curves superpose and there is no hysteresis.

The rate and extent of these changes are the parameters that describe thixotropic behaviour and which can be determined by appropriate rheological experiments.

Generalised Structure Theory

In order to obtain a qualitative description of thixotropic behaviour above yield point, a theory involving a single structure parameter λ has been developed which makes use of the concept of some rheological structure at the molecular and particulate level.[8,9] The time dependence of rheological properties in a thixotropic material is then considered to be due to changes in this structure. Two constitutive equations are used to describe single-structure thixotropic behaviour; a rate equation describing structure breakdown and buildup as a function of shear rate and λ:

$$\frac{d\lambda}{dt} = g(\dot{\gamma}, \lambda) \tag{1}$$

and an equation of state relating shear stress to shear rate and structure parameter λ:

$$\tau = \tau(\dot{\gamma}, \lambda) \tag{2}$$

The simplest form of rate equation for structure breakdown and buildup at constant shear rate is given by Moore: [9]

$$\frac{d\lambda(t)}{dt} = \underbrace{a[1-\lambda(t)]}_{buildup} - \underbrace{b\lambda(t)\dot{\gamma}}_{breakdown} \tag{3}$$

in which it is assumed that the rate of structure breakdown is proportional to both λ and shear rate, whereas the rate of buildup is proportional to the broken structure (1-λ) but is independent of shear rate. This rate equation predicts a dynamic equilibrium when the structure parameter is:

$$\lambda_e = \frac{1}{1+\frac{b}{a}\dot{\gamma}} \tag{4}$$

Moore also suggested an equation of state of the form:

$$\tau(t) = [\eta_\infty + c\lambda(t)]\dot{\gamma} \tag{5}$$

where η_∞ is the viscosity at infinite shear rate and c is the incremental contribution of structure to viscosity. Eq. 5 was later modified by Cheng and Evans [8] who allowed for the presence of a yield stress proportional to the structure parameter λ(t):

$$\tau(t) = \lambda(t)\tau_y + [\eta_\infty + c\lambda(t)]\dot{\gamma} \tag{6}$$

In the case of water-based drilling fluids, there is evidence (Alderman, *et al.*[3], Zamora and Lord [10]) that the equilibrium flow curve is satisfactorily represented by the Herschel-Bulkley equation[11]:

$$\tau = \tau_H + k\dot{\gamma}^n \tag{7}$$

Incorporating the effect of structure on yield stress and viscosity in Eq. 7 gives a modified version of the Moore-Cheng equation (Eq. 5):

$$\tau(t) = \lambda(t)\tau_y + [\eta_\infty + c\lambda(t)]\dot{\gamma}^m \tag{8}$$

Accordingly, the equilibrium flow curve for the modified Moore-Cheng equation becomes:

$$\tau_e = \lambda_e\tau_y + (\eta_\infty + c\lambda_e)\dot{\gamma}^m \tag{9}$$

Equations 3 and 9 may be used as the basis for a mathematical description of thixotropic behaviour in fluids. The various parameters in Eq. 9 can be determined by measuring the steady-state shear stress at a number of shear rates. A plot of τ_e vs. shear rate will then give values for parameters τ_y,

η_∞, c and m in Eq. 9, provided that λ_e can be expressed as a function of shear rate by a relationship such as Eq. 4.

EXPERIMENTAL

Materials

The material used in these experiments was an unweighted WBM containing 64.3 g bentonite per litre of water (supplied by M-I SWACO). This was prepared by adding the clay to water over a period of two minutes while agitating the suspension with a Silverson high-speed mixer. The pH of the suspension was measured to be about 9.5. The suspension was hot-rolled in an API standard roller oven at 100˚C and at an approximate shear rate of 5 s^{-1}, for a period of 48 hr.

Experimental Procedure

Most of the experiments were carried out on a Bohlin VOR rheometer, using the C25 concentric cylinder geometry as the measuring system. The radii of the bob and cup of the geometry were 12.5 and 13.75 mm, respectively, and the bob had a height of 37.5 mm. The Carrimed controlled-stress rheometer was used for yield-stress measurements with concentric cylinder geometry. Prior to each experiment, the material was cold-rolled for one hr at room temperature and at a shear rate of 5 s^{-1}. This had a homogenising effect on the fluid and brought all samples to similar initial shear history. The samples were allowed to rest in the measuring system of the rheometer for ten minutes before measurements began. The sample temperature was maintained at 25 ±0.1°C throughout each experiment.

To minimise sample dehydration during measurements, a thin layer of a viscosity standard oil S60 (supplied by Cannon Instruments Company, USA), with a viscosity of 102.3 mPa·s at 25°C, was placed on the free surface of the sample. A series of early experiments confirmed that the oil film did not affect the rheological properties of the mud to any measurable extent.

Four types of measurements were performed:

1) Stress relaxation experiments: These were carried out to determine the equilibrium stress at a number of shear rates. The sample was sheared at a constant rate for a certain length of time. Some early experiments were allowed to proceed for up to 25 hr. The results from these showed that the stress values became steady after 3-5 hr. Thereafter, most of the experiments were of 6-8 hr duration. The experiments were repeated 3-6 times at each shear rate and showed good reproducibility. The shear rates used were in the range 2.9–1460 s^{-1}.
2) Shear rate step-change experiments: In these measurements the shear rate was held constant at an initial value $\dot{\gamma}_1$ until the shear stress reached a steady final value. Then the shear rate was abruptly changed to a new value $\dot{\gamma}_2$ and the time-dependent shear stress was measured to equilibrium. This procedure was repeated several times between four different pairs of high-low or low-high shear rates. The results of these experiments were used to establish the time- and shear-history dependence of shear stress.
3) Yield stress measurements: These were carried out on the controlled-stress rheometer. Shear stress was applied to the sample and increased at a controlled rate until angular displacement was detected.
4) Hysteresis loops: In these experiments the shear rate was ramped repeatedly at a controlled rate over a selected range and the corresponding shear stress was measured. The aim of these experiments was to obtain the hysteresis loops characteristic of thixotropic materials.

RESULTS AND DISCUSSION

Fig. 3 shows typical stress-relaxation data at several shear rates. The results indicate that there is a relatively sharp drop in shear stress in the early stages of shearing, consistent with a fast initial structure breakdown.

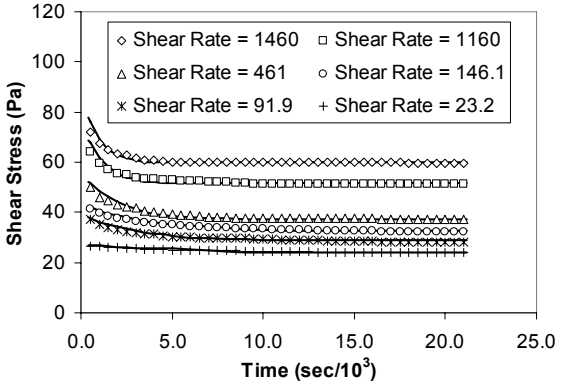

Figure 3. Steady-shear stress-relaxation data.

In most of the experiments, the shear stress reached a steady value τ_e within the duration of the experiment, but at the lower shear rates (<100 s^{-1}) shear stress continued to decline even after 8 hr, suggesting long relaxation times. Subsequently, some of these experiments were repeated during the shear rate step-change measurements such that equilibrium was approached both from above (net breakdown) and from below (net buildup) in order to find the true τ_e.

Fig. 4 is a plot of the equilibrium stress τ_e as a function of shear rate. The data indicate that the material has a finite yield stress and that the change in the slope of the flow curve decreases as the shear rate is increased. This is characteristic of the Herschel-Bulkley type fluids.

An example of the shear rate step-change experiments is illustrated in Fig. 5, where stress relaxation is in the form of decay or recovery depending on whether the shear rate is increased or decreased.

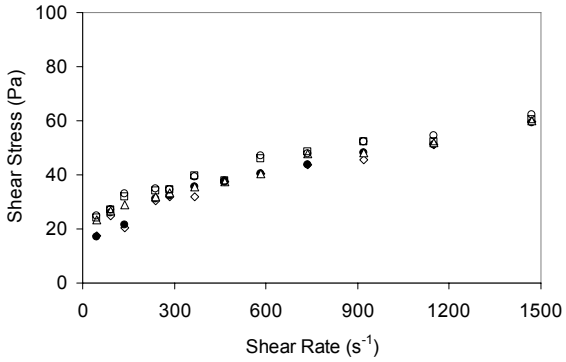

Figure 4. Equilibrium flow curves.

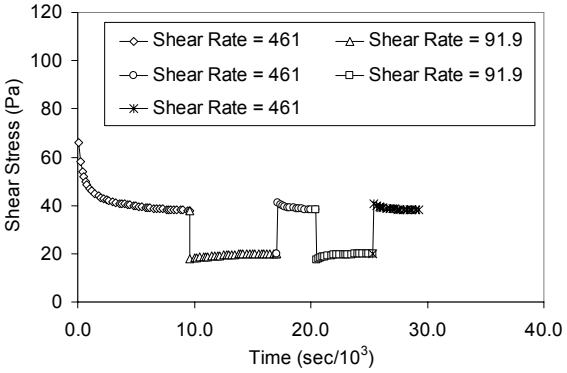

Figure 5. Shear rate step-change tests.

Single-Structure Model

To find the parameters in the modified Moore-Cheng equation (Eq. 8), it is necessary to express λ_e as a function of shear rate. Eq. 4 is one such relationship based on the single-structure theory by Moore (Eq. 3). This theory also yields a single-exponential time dependence for λ (at constant shear rate), obtained by integrating Eq. 3,

$$\lambda(t) = (\lambda_0 - \lambda_e)\, e^{-(\frac{1}{T})} + \lambda_e \qquad (10)$$

where,

$$\frac{1}{T} = a + b\dot{\gamma} \qquad (11)$$

and λ_0 is the level of structure at time $t = 0$. Eq. 10 can be used to define the time

dependence of shear stress when substituted in Eq. 8:

$$\tau(t) = \tau_1 e^{-(\frac{1}{T})} + \tau_e \quad (12)$$

where,

$$\tau_1 = (\lambda_0 - \lambda_e)(\tau_y + c\dot{\gamma}^m) \quad (13)$$

$$\tau_e = \lambda_e \tau_y + (\eta_\infty + c\lambda_e)\dot{\gamma}^m \quad (14)$$

The validity of the single-structure rate equation for the WBM of these experiments was tested by fitting a 3-parameter single-exponential function [τ_1, T and τ_e in Eq. 12] to the experimental shear stress-time data and using a non-analytical least-squares regression routine. These are shown as the solid lines in Fig. 3 for some of the stress-relaxation experiments. Although the general fit is good, it seems that such function does not describe the data satisfactorily at early times in the experiments. This might suggest that in the stress-relaxation experiments, where the material is sheared from rest, *i.e.* a state of relatively high structure, there is a fast viscous drag-driven structure breakdown (to flocs and aggregates) followed by a slower breakdown caused by the collision of mobile flocs and aggregates. Because the population of data points is heavier toward the steady state, it is mostly the behaviour of the slower process that is reflected in the fitted function.

At constant shear rate, the regression coefficient χ^2 may be defined as:

$$\chi^2 = \frac{1}{(N-M)\tau_e^{\,2}} \sum_{i=1}^{N} [\tau(t_i)_{meas.} - \tau(t_i)_{calc.}]^2 \quad (15)$$

in which N is the number of data points and M is the number of parameters in the function to be fitted. For the stress relaxation data, χ^2 ranged from 2.5×10^{-5} at the lower shear rates to 0.02 at the highest shear rate, another indication that the initial breakdown, which is faster at higher shear rates, is not well predicted.

Eq. 12 gives a better average fit ($\chi^2 = 7.0 \times 10^{-5}$) to the shear stress-time data obtained in the rate step-change experiments, because here the material has already been sheared and has a lower level of structure. Consequently, the initial breakdown by viscous drag is less severe, and the single-exponential function gives a closer prediction.

Fig. 6 is a plot of the pre-exponential coefficient τ_1 vs. $\dot{\gamma}$ (Eq. 12). The data exhibit a steep rise with $\dot{\gamma}$ at lower shear rates. A similar behaviour is observed in the plot of T^{-1} vs. $\dot{\gamma}$ (Eq. 11), Fig. 7.

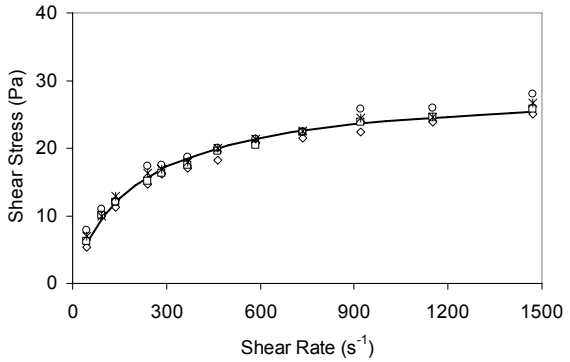

Figure 6. Pre-exponential coefficients from a single-exponential fit to stress-relaxation data.

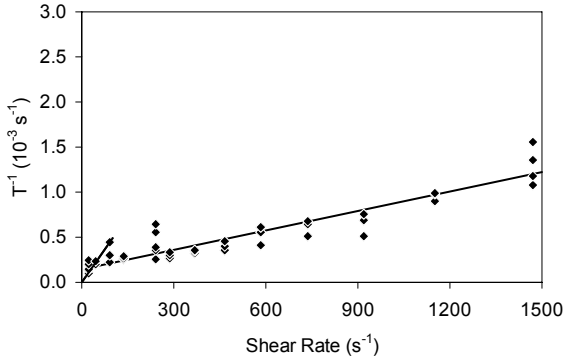

Figure 7. Inverse relaxation time vs. shear rate for stress-relaxation experiments.

Time-Dependence of Shear Stress

According to the single-structure rate theory, the relaxation time decreases with increasing shear rate (Eq. 11); a plot of T^{-1} vs. $\dot{\gamma}$ is a straight line with slope b, and intercept a on the T^{-1} axis. However, it seems from Fig. 7 that at lower shear rates, up to about 100 s^{-1}, the relaxation time decreases sharply with increasing $\dot{\gamma}$ and then follows a slower rate of decrease as shear rate increases.

A method advocated by many for determining the time dependence of shear stress is the high-low shear rate step-change procedure illustrated in Fig. 5. Assuming single-exponential time dependence, a least-squares regression of data at two shear rates gives the time constants for structure breakdown and buildup, T_1 and T_2, respectively:

$$\frac{1}{T_1} = a + b\,\dot{\gamma}_1 \tag{16}$$

$$\frac{1}{T_2} = a + b\,\dot{\gamma}_2 \tag{17}$$

from which the constants a and b are calculated. The range of shear rates used in the step-change experiments was 100–1500 s^{-1}. The results of these experiments are presented in Table 1 as the relaxation times of the breakdown (low-to-high shear rate) and buildup (high-to-low shear rate) processes. The average value of χ^2 for these calculations was 7.0×10^{-5}, and the error in the reported relaxation times was less than 1%. The relaxation times to the left of the diagonal belong to net buildup of structure, while those to the right of the diagonal represent net breakdown.

Table 1. Relaxation times of structure breakdown and buildup processes.

Shear rate (s^{-1})	To			
From	91.9	146.1	461.0	1460.0
91.9	-	-	608	143
146.1	-	-	661	331
461.0	1550	1060	-	671
1460.0	1060	1230	910	-

The results suggest that the buildup of structure is a slower process than the breakdown. In one case (91.9 and 146.1 s^{-1}) the close proximity of the two shear rates made calculation of their relaxation times subject to large errors.

For each pair of relaxation times, Eqs. 16 and 17 were solved simultaneously to find the constants a and b. These are given in Table 2 for five pairs of the shear rates used. Due to the wide variation in the b/a ratio, it is unlikely that the time dependence of the WBM can be adequately described by a single relationship over the entire range of shear rates. A better approximation may be obtained by fitting two straight lines to the T^{-1} vs. $\dot{\gamma}$ data:

For shear rates in the range 0 – 100 s^{-1},

$$\frac{1}{T} = 1.5\times10^{-5} + 4.8\times10^{-6}\,\dot{\gamma} \tag{18}$$

and for 100 – 1500 s^{-1},

$$\frac{1}{T} = 1.5\times10^{-4} + 7.0\times10^{-7}\,\dot{\gamma} \tag{19}$$

The straight lines in Fig. 7 show a graphical representation of the above relationships.

Table 2. Rate constants for structure breakdown and buildup processes.

Shear Rates (s^{-1})	a (s^{-1})	b	b/a (s)
91.9 ↔ 461.0	4.0×10^{-4}	2.7×10^{-6}	0.0068
91.9 ↔ 1460.0	6.5×10^{-4}	4.3×10^{-6}	0.0066
146.1 ↔ 461.0	6.8×10^{-4}	1.8×10^{-6}	0.0026
146.1 ↔ 1460.0	5.7×10^{-4}	1.7×10^{-6}	0.0029
461.0 ↔ 1460.0	9.2×10^{-4}	0.4×10^{-6}	0.0004

In the absence of a single description for time dependence in the range of shear rates used here, the value of the b/a ratio will have to be determined by means of curve fitting to the equilibrium stress data.

Shear-History Dependence of Shear Stress

To describe structure as a function of time, it is necessary to find an expression for λ_0. The initial structure λ_0 depends on the previous shear rate(s) to which the material may have been subjected. Therefore, λ_0 is the parameter that describes the shear-history dependence of the rheological properties. λ_0 cannot be measured directly but it may be determined in terms of τ_1, the pre-exponential coefficient in the time description of stress-relaxation curves, as described below.

Differentiation of Eqs. 8 and 12 with respect to time, and at constant shear rate, gives:

$$\frac{d\tau(t)}{dt} = (\tau_y + c\,\dot{\gamma}^m)\frac{d\lambda(t)}{dt} \tag{20}$$

$$\frac{d\tau(t)}{dt} = -\frac{\tau_1}{T}e^{-(\frac{t}{T})} \tag{21}$$

Eliminating $d\tau(t)/dt$ between Eqs. 20 and 21 leads to:

$$\frac{d\lambda(t)}{dt} = \frac{\tau_1}{T(\tau_y + c\,\dot{\gamma}^m)}e^{-(\frac{t}{T})} \tag{22}$$

Differentiating Eq. 10 in a similar manner gives:

$$\frac{d\lambda(t)}{dt} = \frac{\lambda_0 - \lambda_e}{T}e^{-(\frac{t}{T})} \tag{23}$$

Eliminating $d\lambda(t)/dt$ between Eqs. 22 and 23 results in:

$$\lambda_0 - \lambda_e = \frac{\tau_1}{\tau_y + c\,\dot{\gamma}^m} \tag{24}$$

The τ_1 vs. $\dot{\gamma}$ data presented in Fig. 6 are adequately described by a simple empirical equation of the type:

$$\tau_1 = \frac{k_1\,\dot{\gamma}}{1 + k_2\,\dot{\gamma}} \tag{25}$$

Combining Eqs. 24 and 25 yields,

$$\lambda_0 - \lambda_e = \frac{k_1\,\dot{\gamma}}{(1 + k_2\,\dot{\gamma})(\tau_y + c\,\dot{\gamma}^m)} \tag{26}$$

Parameters in Equilibrium Flow Curve

The parameters τ_y, b/a, η_∞, c and m in Eq. 9 have now to be determined by a combination of curve fitting (of the measured τ_e data to the modified Moore-Cheng model) and independent measurements. The independent measurements are needed to reduce the number of parameters determined by curve fitting so that a unique "best fit" can be determined.

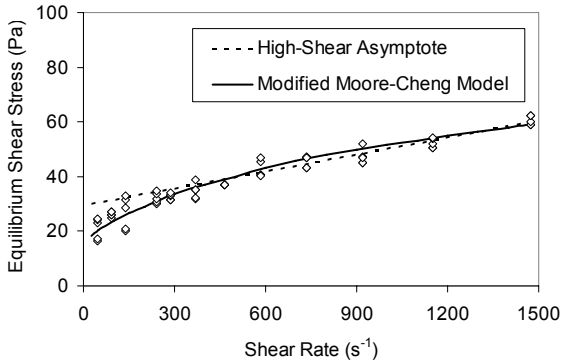

Figure 8. Illustration of the high-shear asymptote and the modified Moore-Cheng model.

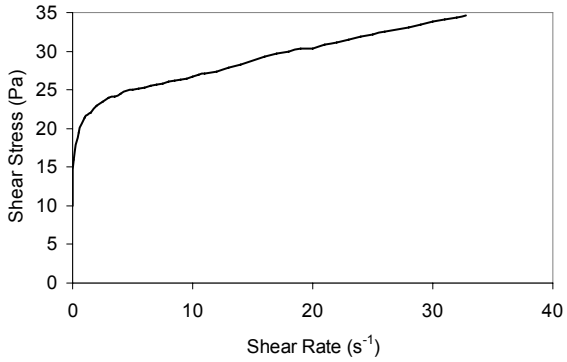

Figure 9. Determination of the yield stress on the controlled-stress rheometer.

One way of achieving this is by assuming that the drilling fluid behaves like a Bingham fluid at higher shear rates, *i.e.* m~1, and that the τ_e vs. $\dot{\gamma}$ data can be approximated by a straight line in that region ($\lambda_0 \sim 0$). The slope of the high-shear asymptote will then give η_∞. Fitting a straight line through the data above $\dot{\gamma}$ = 500 s^{-1} in Fig. 8 gives η_∞ = 0.02 ±0.002. If it is assumed that this is a good estimate for η_∞ in the Moore-Cheng model, then it will have the units $Pa \cdot s^m$.

A second parameter to be determined independently is the yield stress τ_y. This was achieved by using the Carrimed controlled-stress rheometer along with the concentric cylinder geometry. The test fluid was pre-treated in the same way as in all other measurements, *i.e.* 10-min cold-rolling followed by a 10-min rest period to reach thermal equilibrium. The yield stress was determined by applying a known shear stress to the sample and observing the rate of angular displacement. The shear stress was increased gradually until a displacement was detected. The measurements were repeated several times, and a reproducible value of τ_y = 16.0 Pa was obtained (Fig. 9). This value was adopted as the yield stress corresponding to the initial structural state of the fluid as used in all of the experiments.

Substituting for η_∞ = 0.02 $Pa \cdot s^m$ and τ_y = 16.0 Pa, the modified Moore-Cheng equation at steady state becomes:

$$\tau_e = \frac{16.0}{1+\frac{b}{a}\dot{\gamma}} + (0.02 + \frac{c}{1+\frac{b}{a}\dot{\gamma}})\,\dot{\gamma}^m \qquad (27)$$

In the above function, parameters c and b/a exhibit high sensitivity to small variations in the value of m. For example, a 1% change in m produces variations as high as 20% and 30% in c and b/a, respectively. As a result, the function still does not seem to give a single best fit. Since parameters c and b/a have similar mutual sensitivities, it is necessary to force the value of m in Eq. 27.

In the family of the best fits obtained by least-squares regression of the equilibrium data, the value of m varies from 0.642 to 0.985. Assuming an average value of m = 0.81, Eq. 27 may be forced to produce singular values for b/a and c:

$$\frac{b}{a} = 5.44\times10^{-4} \pm 9.46\times10^{-5} \qquad (28)$$

$$c = 0.20 \pm 0.015 \qquad (29)$$

The fitted curve represented by these parameters is illustrated in Figure 8.

The complete set of relationships produced for describing the time- and shear-

history dependence of the rheological properties of the WBM of these experiments is as follows:

$$\tau(t) = \tau_y\, \lambda(t) + [\eta_\infty + c\,\lambda(t)]\,\dot{\gamma}^m \tag{30}$$

$$\lambda(t) = (\lambda_0 - \lambda_e)\, e^{-(\frac{t}{T})} + \lambda_e \tag{31}$$

where,

$$\lambda_e = \frac{1}{1 + \frac{b}{a}\dot{\gamma}} \tag{32}$$

$$\lambda_0 - \lambda_e = \frac{k_1\,\dot{\gamma}}{(1 + k_2\,\dot{\gamma})(\tau_y + c\,\dot{\gamma}^m)} \tag{33}$$

$$\tau_y = 16.0 \tag{34}$$

$$\eta_\infty = 0.02 \tag{35}$$

$$c = 0.20 \tag{36}$$

$$m = 0.81 \tag{37}$$

$$\frac{b}{a} = 5.44\times10^{-4} \tag{38}$$

$$k_1 = 0.145 \tag{39}$$

$$k_2 = 0.00516 \tag{42}$$

and the time dependence is further defined by the following relationships:

For shear rates in the range 0 – 100 s^{-1}:

$$\frac{1}{T} = 1.5\times10^{-5} + 4.8\times10^{-6}\,\dot{\gamma} \tag{43}$$

and for 100 – 1500 s^{-1}:

$$\frac{1}{T} = 1.5\times10^{-4} + 7.0\times10^{-7}\,\dot{\gamma} \tag{44}$$

Prediction of Hysteresis Loops

The validity of the model and the accuracy of the final curve fitting can now be tested by predicting the hysteresis loops produced when the shear rate is ramped. If the fluid is subjected to a sequence of shear rates $\dot{\gamma}_i$, for a period t_i at each shear rate, the structure λ_i at the end of interval i, becomes the initial structure for the next interval at shear rate $\dot{\gamma}_{i+1}$, *i.e.* $\lambda_{0,i+1} = \lambda_i(t_i)$.

The experimental data in Fig. 10 were obtained by ramping the shear rate up and then down over the range 11.6 – 1460 s^{-1}. The cycle was repeated five times. The ramp time, *i.e.* total "up" or "down" time, was 48 min, equivalent to 20 readings at 144-second intervals. The fluid was pre-treated as described earlier. The model was used to predict the level of structure at the end of the time interval at each shear rate. This level of structure then became λ_0 for the next time interval. The same method was followed for both "up" and "down" curves.

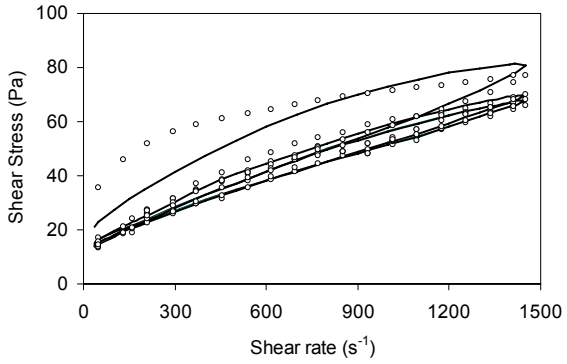

Figure 10. Hysteresis loops produced by ramping the shear rate in the range 14.6-1460 s^{-1}.

The solid lines in Fig. 10 show the calculated hysteresis loops. The model fails to predict the first cycle satisfactorily. This is expected because, as discussed earlier, the single-exponential time dependence does not fit the stress relaxation data well at early times. However, as time progresses, *i.e.* as the cycle is repeated, the agreement between the experimental and predicted values improves. The fourth and fifth cycles practically superpose, indicating that the equilibrium loop (to be distinguished from the equilibrium flow curve) is obtained after a few cycles. The maximum difference

between the measured stress values and those predicted by the model for the final loop is about 7%. This value decreases as the ramp time is increased. For example, a total ramp time of 90 min gave a maximum difference of 5% in the last loop, while a shorter time of 32 min increased the error to 9%.

The slopes of the "up" and "down" curves are determined to a large extent by the value of parameter *m*. It appears that the assumed average value of $m = 0.81$ produces good agreement with the experimental data.

For the model to give a good prediction of thixotropic behaviour, one of the following initial conditions must be satisfied:

1) Material initially sheared at a very high rate so that $\lambda_0 \sim 0$. This corresponds to the condition of the drilling fluid as it issues at the drill bit, where it is subjected to shear rates on the order of 10^5 s^{-1}.
2) Fluid at equilibrium at a finite shear rate such that $\lambda_0 = \lambda_e$. This condition may correspond to the state of the fluid in the circulation system at the surface.
3) Material initially at rest, as in the case when there is a break in fluid circulation. In this situation, one may assume that the initial conditions are the same as those for the fluid in these experiments, or if there has been for an extended break in circulation, one may assume that the fluid has a fully formed structure, i.e. $\lambda_0 = 1$.

ALTERNATIVE THIXOTROPY MODELS

Due to its simplicity, the single-structure theory does not consider the physical and chemical nature of the structure. A more precise model for describing structural processes under shear requires a good knowledge of the nature of structure as well as the type of changes that it undergoes when sheared. An alternative model that may be considered in the absence of such information is one in which structure breakdown and buildup are assumed to be governed by two rate processes with distinctly different relaxation times. In this scheme the first process may be a fast, viscous drag-driven breakdown, which breaks the intact (house-of-cards) structure into flocs and aggregates. The second process has a slower but longer-term effect; it causes further breakdown by promoting collision between the mobile flocs and aggregates and modifies the orientation of the particles thus formed in order to fully accommodate the applied shear stress. Within the remaining intact structure the rate of collision and particle orientation is negligible due to low mobility of the flocs and aggregates. Therefore, the two structural processes may be assumed to be of the consecutive or series type.

The observations made earlier with regard to relaxation time-shear rate relationship for the WBM of this study, favour a two-structure model. In such a model, the time dependence of structure at constant shear rate may be described by a double-exponential function of the type:

$$\lambda(t) = \lambda_1 e^{-(\frac{t}{T_1})} + \lambda_2 e^{-(\frac{t}{T_2})} + \lambda_e \qquad (43)$$

in which the coefficients λ_1, λ_2, λ_e, T_1 and T_2 are functions of shear rate. A similar function describing the time dependence of shear stress at constant shear rate was fitted to the stress relaxation data of this study, and the values of χ^2 were found to be better, at least by a factor of two, than those obtained with the single-exponential function. Mathematical derivations leading to the time-description of structure have been made for this model, and it appears that the five coefficients involved in Eq. 43 are complicated functions of shear rate which do not lend themselves to determination by simple optimisation procedures. This makes the two-structure model unsuitable for engineering applications.

CONCLUSIONS

The thixotropic characteristics of some drilling fluids may have a significant effect on their rheological properties in the time scale and range of shear rates encountered around the wellbore. Hitherto, the effect has been accounted for in fluid design and engineering calculations by the 10-sec and 10-min gel values measured routinely in drilling fluid laboratories. The results of this work show that relatively simple semi-empirical models, based on a single-structure theory, may be devised in such a way that the effects of time and shear history on rheology can be incorporated in engineering calculations.

Although this model is based on an unweighted bentonite suspension, similar work on weighted muds may be carried out in order to study the effect of added solids on thixotropic behaviour. There is scope for further work to determine the temperature dependence of such behaviour, as well as its nature and effect in turbulent flows.

ACKNOWLEDGMENTS

The author thanks M-I SWACO for permitting the publication of this work.

REFERENCES

1. Jenekhe, S.A., Davis, H.T. and Scriven, L.E. (1989), "Cold Stage Scanning Electron Microscopy of Bentonite Suspensions," 38th Annual Proceedings of Electron Microscopy Society of America, (Ed. G.W. Bailey), San Francisco, California, 206.

2. Dairanieh, I.S. and Lahalih, S.M. (1988), "Novel Polymeric Drilling Mud Viscosifiers," *Euro. Polym. J.* **24**, 831.

3. Alderman, N.J., Ram Babu, D., Hughes, T.L. and Maitland, G.C. (1988), "The Rheological Properties of Water-Based Drilling Fluids," 10th International Congress on Rheology, Sydney, August 14-19.

4. Annis, M.R. (1967), "High-Temperature Flow Properties of Water-Based Drilling Fluids," *J. Pet. Tech*., **19** (8), 1074.

5. Hiller, K.H. (1963), "Rheological Measurements on Clay Suspensions and Drilling Fluids at High Temperatures and Pressures," *J. Pet. Tech.,* **15** (7), 779.

6. Mercer, H.A. and Weymann, H.D. (1974), "Structure of Thixotropic Suspensions in Shear Flow. III. Time-Dependent Behaviour," *Trans. Soc. Rheol.,* **82** (1), 199.

7. Dolz, M., Jiménez, J., Jésus Hernández, M., Delegido, J. and Casanovas, A. (2007), "Flow and Thixotropy of non-Contaminating Oil Drilling Fluids Formulated with Bentonite and Sodium Carboxymethyl Cellulose," *J. Pet. Sci. Eng.* **57**, 294-302.

8. Cheng, D.C-H. and Evans, F. (1965), "Phenomenological Characterisation Of The Rheological Behaviour of Inelastic Reversible Thixotropic and Anti-Thixotropic Fluids," *Brit. J. Appl. Phys.,* **16**, 1599.

9. Moore, F. (1959), "The Rheology of Ceramic Slips and Bodies," *Brit. Cream. Soc. Trans.,* **58**, 470.

10. Zamora, M. and Lord, D.L. (1974), "Practical Analysis of Drilling Mud Flow in Pipes and Annuli," *SPE 4976,* 49th Annual Fall Meeting of the Soc. Pet. Eng.

11. Herschel, W.H and Bulkley, R. (1926), "Measurement of Consistency as Applied to Rubber-Benzene Solutions" *Proc. Amer. Soc. Test. Mat.,* **26**, 621.